Swelling Dynamics of Ultrathin Films of Strong Polyelectrolytes

ARTICLE *in* MACROMOLECULES · APRIL 2011

Impact Factor: 5.8 · DOI: 10.1021/ma200240t

2 AUTHORS:

Tanusree Samanta
Haldia Institute of Technology
5 PUBLICATIONS **5** CITATIONS

SEE PROFILE

Manabendra Mukherjee
Saha Institute of Nuclear Physics
98 PUBLICATIONS **874** CITATIONS

SEE PROFILE

Macromolecules

ARTICLE

pubs.acs.org/Macromolecules

Swelling Dynamics of Ultrathin Films of Strong Polyelectrolytes

Tanusree Samanta and M. Mukherjee*

Surface Physics Division, Saha Institute of Nuclear Physics, 1/AF Bidhannagar, Kolkata 700064, India

ABSTRACT: Solvent mass uptake and the swelling of ultrathin polyelectrolyte films (within thickness range 157−375 Å) in the presence of water vapor have been performed to study the effect of long-range Coulombic interaction between charged segments of a polyelectrolyte chain on its swelling dynamics. Films were prepared from aqueous solution of poly(sodium 4-styrenesulfonate) (NaPSS) on hydrophilic silicon substrate using the spin-coating method. Diffusion coefficient of water has been obtained from the solvent mass uptake study using gravimetric measurement and was found to increase with the increase of film thickness. Swelling dynamics of the polymer films in the presence of water vapor, on the other hand, have been studied in situ using the X-ray reflectivity technique. The diffusion coefficient of the NaPSS chains has been found to be of the order of 10^{-18} cm^2/s and was independent of the film thickness, whereas the fraction of charged monomer which determines the strength of the repulsive interaction between the polymer segments shows the confinement effect and increases linearly with the film thickness.

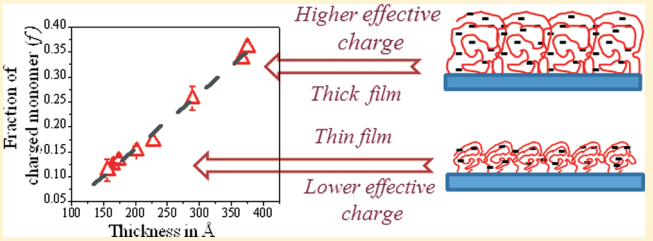

1. INTRODUCTION

In recent years ultrathin polymeric films have drawn tremendous application in the fields of coating, membrane, sensors, etc. Confinement of the polymer leads to the changes in the equilibrium structural and dynamical behaviors of the polymer chains close to the substrate[1−5] due to energetic interactions between polymer chains and the substrate. When a dry polymer is exposed to a solvent, the solvent molecules enter through the porous structure of the polymer. If the solvent is a good solvent for the polymer, there is a strong attractive interaction between the polymer and the solvent, and the net interaction between the polymer segments is repulsive. As a result, the polymer molecule starts to swell. The understanding of the mobility of the polymer chains and their equilibrium structure close to the substrate or interfaces in the presence of solvent vapor are of technological importance in many areas like emulsion, coating, and adhesion.[6] The phenomenon of solvent absorption into the pores of polymer has been exploited by several authors to study the diffusion of solvent into the pores,[7,8] pore size distribution,[9,10] viscoelastic properties,[11,12] etc.

In our previous studies,[13−17] we have presented the swelling dynamics of water-soluble neutral polymer films where the effects of various interactions on swelling dynamics have been studied extensively. Those results show that the diffusion coefficient of polymer chains in D_2O vapor is 1 order of magnitude faster when compared to their dynamics in H_2O, indicating the effect of polymer−solvent interaction on chain mobility.[14] Again, polymer−substrate attachment in annealed polymer films makes the dynamics of the restricted part of polymer chains 1 order slower than its free part and swellability of the film decreases with increase of annealing temperature.[15] Also, the polymer−particle interaction in polymer nanocomposite thin films modifies the overall dynamical behavior of the films since a fraction of polymer chains, directly attached to the nanoparticles, lose their freedom of motion.[16,17] The results indicate that swelling dynamics is sensitive to the minute changes in polymeric system or polymer−solvent interaction.

Polyelectrolytes are charged macromolecules which ionize in the presence of polar solvents like water. A long-range Coulomb interaction between the charged polymer segments comes into play which is absent in neutral polymer. The Coulombic interaction modifies the behavior of bulk polyelectrolyte solutions as observed in the change in their crossover concentrations,[18] osmotic pressure of the polyelectrolyte solution,[19] or dependence of solution viscosity on the polymer concentrations.[20,21] The adsorption of polyelectrolyte chains on a neutral surface is also different from that of neutral polymer and has a strong dependence on the charge density of the chains, concentration of the salt present, etc.[22] These factors also affect the dynamics of polyelectrolyte chains[23] and the growth of polyelectrolyte multilayer.[24] Apart from that, many natural polymers like protein and DNA also belong to the family of polyelectrolytes, and the Coulomb interaction in these systems plays an important role in biological phenomenon like binding of protein to the membrane,[25] adsorption of DNA on the surface of a supported lipid membrane,[26,27] etc.

In our present study a strong polyelectrolyte poly(sodium-4-styrenesulfonate) (NaPSS) is used for the study of swelling dynamics of ultrathin polyelectrolyte films. Here we discuss the solvent mass uptake and swelling dynamics of spin-coated polyelectrolyte films at saturated water vapor pressure conditions. The gravimetric method was used to study the dynamics of

Received: February 2, 2011
Revised: March 28, 2011
Published: April 15, 2011

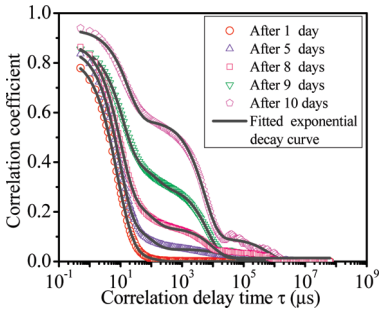

Figure 1. Intensity−intensity autocorrelation function for solution of concentration 12 mg/mL obtained from dynamic light scattering. Different symbols represent the data taken at different times. The data were fitted with sum of three exponential decay functions represented by solid lines.

water molecules in the polymer films, whereas swelling dynamics of the polymer chains were studied using the X-ray reflectivity technique. Compared to our previous swelling study with neutral polymer,[13] the diffusion coefficient of the charged polymer chains was observed to be more than 1 order of magnitude smaller. The saturated swelled thickness was also found to be larger compared to that of neutral polymer. Moreover, the fraction of charged monomers of the polyelectrolyte chains, which plays a similar role as that of excluded volume for neutral polymer, was thickness dependent and decreases with increase of confinement of the polyelectrolyte films.

2. EXPERIMENTAL SECTION

2.1. Dynamic Light Scattering. NaPSS (30% water solution) was procured from Sigma-Aldrich (molecular weight 2×10^5). It was observed that there is a tendency of agglomeration of polyelectrolyte chains in dilute solutions with time. Therefore, it was necessary to determine the chain morphology in the starting solution in order to find an optimum condition of the same to prepare all the films from similar morphological conditions. Before preparation of ultrathin films the morphology and dynamics of the chains in the NaPSS solution was studied by dynamic light scattering (Zetasizer Nano-S, Malvern instrument). The intensity−intensity time correlation (autocorrelation) data for aqueous solution of NaPSS of different concentration ranging from 3 to 30 mg/mL were taken regularly for 25 days at a regular interval. According to the phase diagram,[28] all the solutions were in semidilute regime (overlap concentration ~0.8 mg/mL). Figure 1 shows the time dependence of the autocorrelation function for solution of concentration 12 mg/mL as a typical case.

The figure indicates that the nature of intensity autocorrelation function changes (showing multimodal decay) with time. If the polymer chains are homogeneously dissolved in the solvent, the correlation function is likely to show a single-exponential decay behavior. The presence of multiple time constants in the present case indicates partial agglomeration or cross-linking of the polymer chains which make the solution heterogeneous.[29] Therefore, the variation of autocorrelation function with time shows change in solution morphology as time progress. The agglomeration time was found to be dependent on the solution concentration. To compare the behavior of different correlation data for different concentrations, all the autocorrelation functions $g_2(\tau)$ are fitted with a sum of three exponential decay functions given by $g_2(\tau) = A_1 \exp(-\tau/t_1) + A_2 \exp(-\tau/t_2) + A_3 \exp(-\tau/t_3)$ as shown in Figure 1, where t_i's are proportional to the agglomerate size ($t_1 < t_2 < t_3$) and A_i's represent their weight factors.

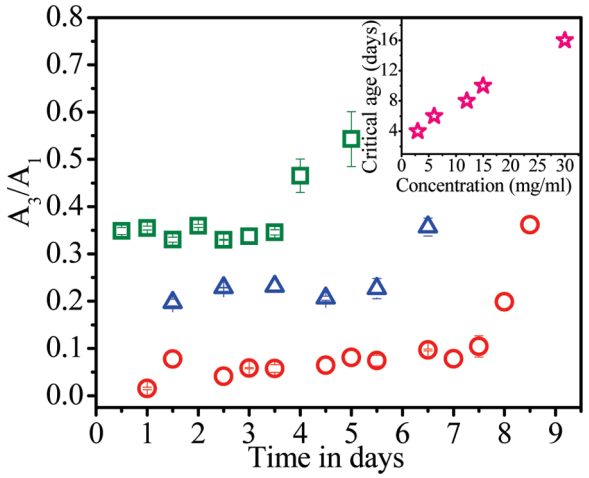

Figure 2. Variation of A_3/A_1 ratio with age of the solutions. The symbols square, triangle, and circle respectively represent the concentrations 3, 6, and 12 mg/mL. For clarity, data for lower concentrations are shifted upward. Inset shows the variation of critical age with the solution concentration.

As A_1 and A_3 represent the concentrations of the smallest and the largest agglomerates, respectively, we define the quantity A_3/A_1 as a measure of solution agglomeration. In Figure 2 we have plotted A_3/A_1 as a function of age of the solution for different polymer concentrations.

It is interesting to note that for all the cases the value of A_3/A_1 remains around 0.05 for several days. The value suddenly starts to increase at a particular time. This critical age was found to be a function of polymer concentration in the solution, and inset of the Figure 2 shows the variation of agglomeration time with the solution concentration for all the samples. The ages of the polymer solutions used for preparation of spin-coated films were below their critical age.

2.2. Sample Preparation. Aqueous solutions of poly(sodium 4-styrenesulfonate) of concentrations 24 and 30 mg/mL were prepared by diluting the 300 mg/mL mother solution and were used for film preparation. Thin films of NaPSS were prepared on silicon(100) substrate by the spin-coating technique. Before spin-coating, silicon substrates were cleaned by the RCA cleaning method. In this method the wafers are boiled at 100 °C in a solution of water, ammonium hydroxide, and hydrogen peroxide (H_2O:NH_4OH:H_2O_2 = 2:1:1) for 10 min and rinsed thoroughly with Millipore water. This chemical treatment also enhances the hydrophilicity of the silicon surface by introducing −OH dangling bonds on the surface which helps in better attachment for the water-soluble polymer. Films of different thickness were prepared in ambient condition using spinning speed in the range 3500−5500 rpm. It may be noted that from a single solution of any one concentration films of wide thickness range could not be obtained. Therefore, two different concentrations were used to cover a wider range of thickness. From the 24 mg/mL solution films of thickness within the range 157−228 Å were obtained, whereas from 30 mg/mL solution thicker films of 290−375 Å were prepared.

2.3. Gravimetric Measurement. Mass uptake study of the films has been perfomed using a microbalance (Mettler Toledo, XP6) of microgram mass resolution. Initially, the weight of the dry film (w_0) was recorded. Thereafter, a water container was placed inside the weighing chamber, and the weight of the film (w_t) was recorded as a function of time. Thus, the mass uptake (M_t) of the film at any instant of time (t) in the presence of water vapor is proportional to $w_t - w_0$. It was observed that the RCA cleaned substrate also adsorbs some amount of water. Therefore, the data of mass uptake of the clean substrate was subtracted from that of the film to get the actual mass uptake of the pure NaPSS films.

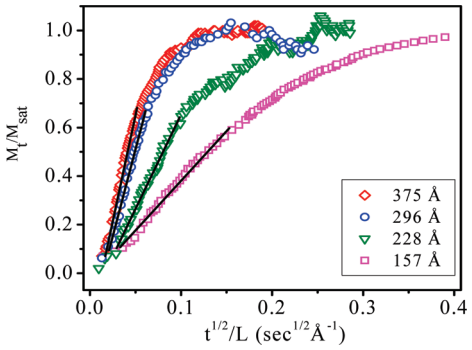

Figure 3. Normalized mass uptake against square root of time scaled with initial thickness (L) of the films. The initial thicknesses of the films are shown against the symbols. Solid lines represent the linear fits to the data.

2.4. X-ray Reflectivity. The specular X-ray reflectivity (XRR) technique is a powerful nondestructive tool which gives information about the thickness and structure of thin films and multilayers. Here we have used this technique to study the swelling dynamics of the thin NaPSS films. X-ray reflectivity data were collected in our laboratory setup using Cu Kα radiation obtained from the copper-sealed tube anode (Bruker AXS, D8 Discover) followed by a Göbel mirror. Specular X-ray reflectivity scans, keeping the incident and reflected angle the same, are taken as functions of momentum transfer vector normal to the surface $q_z = (4\pi/\lambda)\sin\theta$, where θ is the incident and exit angle. The XRR data provide information about the film thickness and the variation of electron density along the depth direction. Initial thickness of the films is measured by placing the sample in a homemade sample cell and maintaining a rotary vacuum ($\sim 5 \times 10^{-2}$ Torr) within the cell as described earlier.[13] To study the swelling of the films, a small water container was inserted within the sample cell so that the films can swell in the saturated water vapor condition, and the change in thickness was monitored in situ using the XRR technique. X-ray reflectivity data during swelling were taken by judiciuslly adjusting of the scan speed and increment in angle so that a sufficient number of thickness oscillations can be obtained within ~10 min, during which the data are collected for each thickness.

3. RESULTS AND DISCUSSION

3.1. Diffusion of Water. In Figure 3, normalized mass uptake (M_t/M_{sat}), normalized by saturated value of mass uptake (M_{sat}), for films of different thickness (L) are shown as a function of $t^{1/2}/L$. It can be observed from the figure that the initial parts (from 0.1 to 0.6) of the curves for all thicknesses are linear. Assuming the Fickian formula for the mass uptake, mass increase for a thin film on an impermeable substrate can be written as[30]

$$\frac{M_t}{M_{sat}} = 2\left(\frac{D_w t}{L^2}\right)^{0.5}\left(\frac{1}{\pi^{0.5}} + 2\sum_{n=1}^{\infty}(-1)^n \,\mathrm{ierfc}\,\frac{nL}{2(D_w t)^{0.5}}\right) \quad (1)$$

where D_w is the diffusivity of water. In this case the water diffusion is assumed to be one-dimensional along the surface normal which is valid for nanoscale thin films.

For short time the expression can be simplified as

$$\frac{M_t}{M_{sat}} = \frac{2}{L}\sqrt{\frac{D_w t}{\pi}} \quad (2)$$

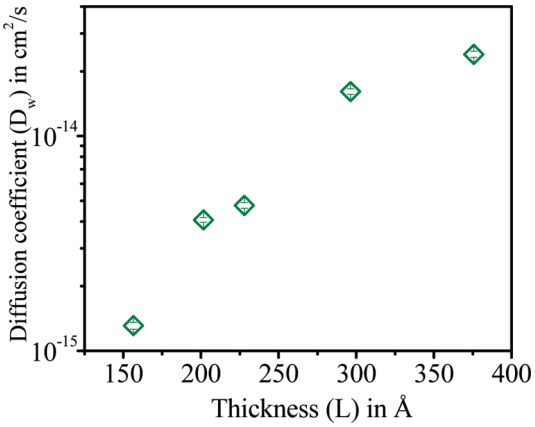

Figure 4. Change of diffusion coefficient of water with film thickness.

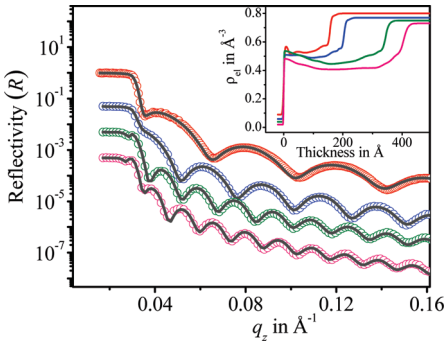

Figure 5. Reflectivity data (symbols) with fitted profiles (lines) during the swelling of polymer films, from top to bottom as increasing swelling time. Top-most data is the reflectivity of the dry film. Inset shows corresponding electron density profiles (ρ_{el}). Data are shifted for clarity.

Considering the linearity of normalized mass uptake at the initial stage, the diffusion coefficient of water (D_w) can be obtained from the slope of the curve by fitting a straight line to the linear part of the M_t/M_{sat} vs $t^{1/2}/L$ data as shown in Figure 3.

It is clear from Figure 3 that the curves corresponding to different thickness do not coincide, indicating thickness-dependent diffusion of water. Figure 4 shows the variation of D_w as a function of initial film thickness (L). One can clearly observe from the figure that the water diffusivity in polyelectrolyte ultrathin films decrease with decreasing film thickness. A similar confinement effect of diffusion coefficient of water in polyelectrolyte films was also observed by Vogt et al.[31] The variation of D_w with film thickness may be explained here in terms of the change in the internal structure of the films due to confinement of the chains between the interfaces. With increasing confinement, the polymer segments get aligned along the substrate which reduces the diameter of the diffusing channels.[14] Hence the diffusion of solvent into these channels is hindered in thinner films as compared to the thicker ones.

3.2. Swelling of the Films. In Figure 5 we have shown the XRR data for a typical film taken at dry state and at the intermediate stages of swelling. It can be observed from the data that number of oscillations in a fixed q_z range increase with time which implies that the thickness of the films also increase with time in presence of water vapor.

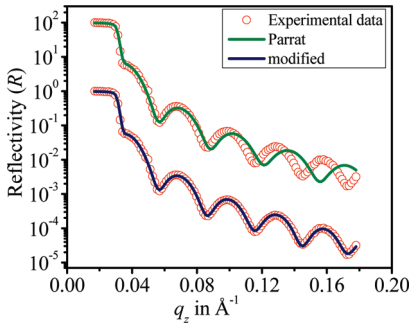

Figure 6. Fitting of XRR data using usual Parrat and the modified formalism.

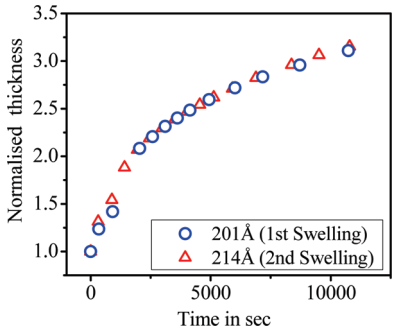

Figure 7. Change of film thickness with time for a typical film during first and second cycle of swelling. Thicknesses during swelling are normalized by their respective initial dry thickness.

The reflectivity data were analyzed using Parrat formalism,[32] modified to include interfacial roughness,[33] to obtain the thickness and the electron density along the depth direction for all the films. To analyze the data using this formalism, the polymer films are virtually divided into many layers with each thickness greater than the depth resolution ($2\pi/q_{max}$, where q_{max} is the maximum range of wave vector transfer for a given set of reflectivity data) of the experiment, and the data are fitted taking thickness, electron density, and roughness of various layers as fitting parameters.

It is interesting to note that during swelling each reflectivity scan is taken in a dynamic condition where the film thickness changes with time. Therefore, for some of the swelling data it becomes difficult to get a good fit with a single film thickness. To overcome this problem, we have devised the following scheme to analyze the data. In this modified analysis scheme we have introduced the effect of time in thickness change during a single scan through the parameter q_z (as q_z also changes monotonically with time). As a first approximation the thickness of each layer was taken as a linear function of q_z. Mathematically, $d(i) = d_{ini}(i) + sq_z$, where $d_{ini}(i)$ and $d(i)$ are thickness of the ith layer at initial time of data acquisition for that particular scan and any other instant of time, respectively. The slope s was taken as a fitting parameter, and to limit the number of parameters, the same value of slope was used for all the layers. A substantial betterment of fitting was achieved using this technique as shown in Figure 6.

Fitted XRR data and corresponding electron density profile for a typical NaPSS film are shown in Figure 5. It may be noted that there is a tendency for the NaPSS films to get dewetted on prolonged swelling, and therefore preswelling of the films to release the residual strain was not performed before the swelling experiments. However, to investigate the effect of preswelling

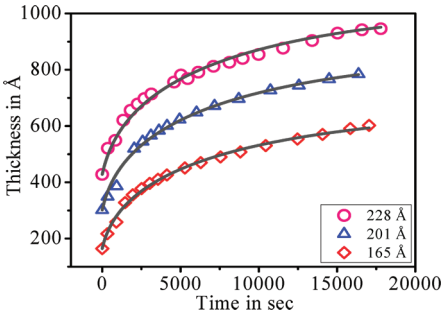

Figure 8. Change of the film thickness in presence of water vapor as a function of time. Data for three films of different thicknesses are represented against different symbols. Solid lines are obtained by fitting the data with eq 5. For clarity, curves for different thicknesses are shifted upward.

on the swelling dynamics, an experiment was performed in two successive dry to wet cycles with two films of different thicknesses (157 and 201 Å). For both the films dry thickness for the second cycle was found to be slightly larger than that of the first which may be due to incomplete drying of the films.

In Figure 7 we have plotted the thicknesses of one film during the two swelling cycles normalized by their respective initial dry thickness. It is clear from Figure 7 that the swellings of the film during two successive cycles are identical. The swelling parameters obtained from the two cycles were also identical for both the films. This indicates that a preswelling treatment for reduction of stress was not required for these films as the effect of residual strain was negligible in case of swelling dynamics for polymer films.

3.3. Dynamics of Polymer Chains. In Figure 8 we have plotted the film thickness as obtained from XRR data taken during swelling as a function of swelling time for films of three different thicknesses.

To analyze the data, we consider the following model for swelling of the polyelectrolyte films. Since the concentration of the solutions from which the films were prepared lie well within the semidilute regime,[28] the polyelectrolyte films are assumed to be formed by the placement of segregated coils on the substrate,[34] and in the presence of solvent vapor each coil would swell independently. The swelling dynamics in this case can be explained in terms of dissipative equation of motion for the end to end distance (R) of a single coil given by

$$\frac{\partial R}{\partial t} = -\mu \frac{\partial F(R)}{\partial t} \tag{3}$$

where $F(R)$ is the free energy and μ is the mobility of the chain.

Here we consider Flory-like free energy for the polyelectrolyte chains as proposed by Kuhn et al.,[35,36] which contains an entropic term and a long-range Coulombic interaction energy term given by

$$F(R) = k_B T \left[\frac{R^2}{Nb^2} + \frac{l_B f^2 N^2}{R} \right] \tag{4}$$

The Coulombic interaction energies of the order of $e^2/4\pi\varepsilon\varepsilon_0 R$ arise from the repulsive interaction between $(Nf)^2$ ion pairs within a chain of diameter of the order of R. Here, N (=970) represents the degree of polymerization, f is the fraction of charged monomers for a particular chain, and l_B is the Bjerrum

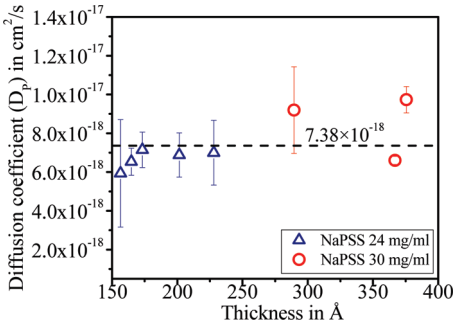

Figure 9. Variation of diffusion coefficient of polyelectrolyte chains with film thickness. Dashed line indicates the average value. Triangles and circles respectively represent the films prepared from solution of concentration 24 and 30 mg/mL.

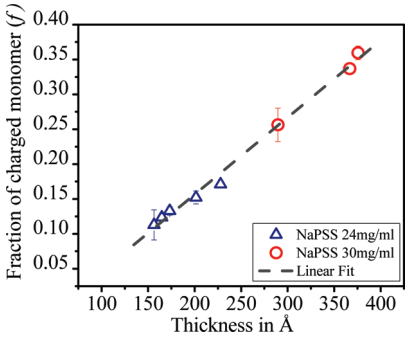

Figure 10. Variation of fraction of charged monomer of the polyelectrolyte chain with film thickness. Triangles and circles respectively represent the films prepared from solution of concentration 24 and 30 mg/mL. Dashed line represents the linear fit to the data.

length defined as the distance at which the electrostatic interaction between two elementary charges in the medium with dielectric constant ε is equal to the thermal energy k_BT ($l_B = e^2/4\pi\varepsilon\varepsilon_0 k_BT$). The term f is related to the linear charge density of the chain and hence decides the strength of the repulsive force between the charged segments. Therefore, it plays a role similar to that of the excluded volume parameter in the case of neutral polymer. In comparison to the long-range electrostatic interaction, the short-range excluded volume contribution to the free energy is neglected here.

In case of thermal motion[37] or during swelling of thin polymer films[13−17] the movement of the polymer chains is observed to be occurring only along the direction perpendicular to the substrate due to physical restriction in the other two in-plane directions. Combining eq 3 and eq 4 and solving the differential equation in one dimension, one can get the following expression for the end to end distance of the polymer chains as a function of time.

$$R(t) = e^{-2D_p t/Nb^2}\left[R_0^3 + \frac{l_B f^2 N^3 b^2}{2}(e^{6D_p t/Nb^2} - 1)\right]^{1/3} \quad (5)$$

where $R_0 = R(t=0)$ and D_p is the diffusion coefficient of the polymer chains related to the chain mobility μ given by the Einstein relation $D_p = \mu k_BT$. Equation 5 was used to fit the experimentally obtained swelling curves as shown in Figure 8. The diffusion coefficient D_p and the fraction of charged monomer f are used as free parameters for fitting. The value of b was

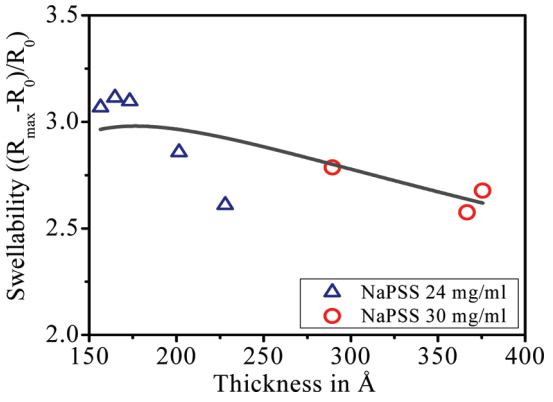

Figure 11. Swellability of polyelectrolyte films as a function of film thickness. Triangles and circles respectively represent the films prepared from solutions of concentration 24 and 30 mg/mL, respectively. Solid line shows the theoretically obtained swellability curve using eq 6.

taken as 2.5 Å, which is average monomer length for vinyl-like polymers,[38,39] and l_B (= 7.12 Å) was calculated for water molecules at room temperature.

In Figure 9 we have plotted the diffusion coefficient of the polymer chains (D_p), as obtained from the fitting, as a function of film thickness. No systematic variation of D_p was observed with film thickness. The average value of the diffusion coefficient was observed to be 7.38×10^{-18} cm^2/s.

Variation of the other fitting parameter, the fraction of charged monomer f, with film thickness is shown in Figure 10. It may be noted that the maximum value of f obtained here was larger than that predicted by Manning−Oosawa counterion condensation theory (0.33 for NaPSS). This theory has been derived assuming the infinite rodlike conformation of polyelectrolyte chains and cannot be exactly applicable for NaPSS which is a flexible polyelectrolyte.[40] Morover details experimental studies[41] show that the limit for the ion condensation for flexible polyelectrolyte chains may be around 45%. This indicates that the value of f greater than 0.33 may be possible in our case. It is interesting to note that the fraction of charged monomer which determines the strength of the repulsive term increases systematically with film thickness. It is well-known that the in-plane component of the radius of gyration of a polymer chain increases with the confinement of the polymer coils when the thickness of the films are reduced.[14,42,43] With flatening of the spheroidal coils along the in-plane direction, attractive interaction between charges on the polymer chains with the free counterions in the solution becomes stronger.[44] Therefore, while the condensed counterions are already attached to the polyelectrolyte coils in the solution due to counterion condensation, the free counterions present in the solution adsorb more on the chains, during preparation of thinner films compared to the thicker ones. As a result, the effective charge of the polyelectrolyte chain decreases with increasing confinement. Another important fact is that the metal ions are hydrophilic in nature.[45] Thus, the free sodium counterions in the solution are likely to feel an attractive interaction toward the hydrophilic silicon substrate. This may give rise to excess counterion density toward the substrate. Therefore, the effective counterions present in the vicinity of the thinner films would be larger compared to the thicker ones. As a result, screening of the polymer charges by the surrounding counterions becomes stronger in thinner films due to closeness of the

polymer chains to the substrate. It may be assumed that the effect of either one or the combination of both reasons described above may be responsible for the decreasing f with the decrease in film thickness.

The total normalized change of film thickness due to swelling may be measured as swellability of the chains defined as $(R_{max} - R_0)/R_0$, where R_{max} is the saturated thickness of the films. Since we cannot take the swelling data up to saturation level as polyelectrolyte films show a tendency to dewet, the film thickness for a very long time was simulated using eq 5 with the fitted values of parameters and was taken as saturated thickness (R_{max}). In Figure 11 we have plotted the swellability for the two sets of films used in the study. The number was found to vary within 2.5−3.1 for all the films showing a systematic dependence of swellabilty on film thickness. As mentioned above, the saturated thickness (R_{max}) depends on the fraction of charged monomer (f) following the relation $R_{max} = cf^{2/3}$, where $c = (l_B N^3 b^2/2)^{1/3}$ is a constant. As we observe, the linearity of f with initial film thickness R_0 in our experimental range we may write $f = f_1 + m(R_0 - R_1)$, where f_1 is the value of f at $R_0 = R_1$, which is the lower limit for our data range and m is the slope. Replacing the expression for f and R_{max} in the expression for swellability, we obtained the following relation:

$$\text{swellability} = \frac{c[f_1 + m(R_0 - R_1)]^{2/3}}{R_0} - 1 \qquad (6)$$

With the value of f_1 and m, as obtained from the straight line fitting of the data shown in Figure 10, and calculated value of c, we have ploted eq 6 as a function of R_0 in Figure 11 along with the experimentally obtained swellability. Although eq 6 does not provide any extra information about the polyelectrolyte, it is worth noting that for linearly increasing f swellability is a nonlinear decreasing function. The figure also indicates that the latter is a more sensitive parameter compared to the former when deviations of data from the functional form (line) are compared with that of Figure 10.

In Figure 12, the diffusion coefficient of water (D_w) and that of polyelectrolyte chains (D_p) have been plotted against film thickness for comparison. One can clearly observe from the figure that D_w is 2−3 orders of magnitude higher that D_p, which implies that diffusion of water for the polyelectrolyte films is a much faster process as compared to the diffusion of polyelectrolyte chains itself. Moreover, diffusion of water shows thickness dependency whereas polyelectrolyte chains do not.

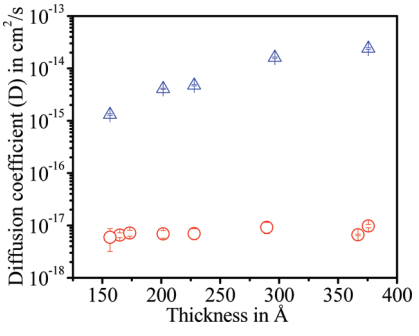

Figure 12. Diffusion coefficient of water (△) and diffusion coefficient of polyelectrolyte chains (○) as a function of film thickness.

3.4. Comparison with Neutral Polymer. It may be interesting to compare the swelling behavior of the strong polyelectrolytes with that of a water-soluble neutral polymer for completeness of the study. In Table 1, we have compared various parameters for NaPSS along with those for polyacrylamide (PAM) obtained from our earlier observation.[13] From the table one can note that the average diffusion coefficient of the polyelectrolyte chains obtained from the analysis of swelling curve was of the order of 10^{-18} cm^2/s while that for PAM, a neutral water-soluble polymer, was of the order of 10^{-16} cm^2/s. This difference in the diffusion coefficient suggests that the confined charged polymer chains undergo a slower dynamics compared to the neutral polymer. This may be explained in terms of the presence of long-range electrostatic interaction in this polymer. Because of this interaction, the diffusing chains are not free as they are there in neutral polymer; rather, they are subjected to some constraint imposed by the surrounding chains through the long-range Coulombic interaction.[46]

The dimensionless coefficient of the repulsive term for polyelectrolyte NaPSS ($l_B f^2 b^2/{R_0}^3$) has been compared with similar repulsive parameter $\nu/{R_0}^3$ for neutral polymer PAM in the table. It is interesting to note the orders of magnitude difference between the two cases. This clearly demonstrates the importance of long-range Coulombic interaction over the short-range van der Waals type repulsive interaction for polyelectrolytes. The water diffusion coefficients for the two systems are also presented in the table. The numbers show that they are constant for neutral polymer, whereas they have a thickness dependency for polyelectrolytes.

4. SUMMARY AND CONCLUSIONS

In the present article we have investigated the swelling of the ultrathin polyelectrolyte films prepared on hydrophilic silicon substrate by the spin-coating method and studied the effect of intrachain long-range electrostatic force on the swelling dynamics. DLS study of the polyelectrolyte solution confirms that the solutions from which the films are prepared are almost free from aggregation. Although the moisture absorption of the polyelectrolyte films was non-Fickian, the diffusion coefficient of water was calculated from the slope of the initial linear part of the M_t/M_{sat} vs $t^{1/2}/L$ curve. The diffusion coefficient of water shows a strong dependence on film thickness and decreases with the confinement of the films. This was attriburted to smaller length and reduced diameters of diffusing channels in thinner films. To explain the swelling dynamics, the change of thickness of the films with time during swelling was modeled in terms of swelling of free polyelectrolyte coils having Flory-like free energy containing entropic contribution and a long-range electrostatic

Table 1. Comparisons of Various Parameters Related to Swelling Dynamics of Neutral Water-Soluble Polymer (PAM) and Strong Polyelectrolyte (NaPSS) Thin Films

	thickness range (Å)	diffusion coefficient of polymer (D_p)	normalized excluded volume ($\nu/{R_0}^3$) or coefficient of repulsive term ($l_B f^2 b^2/{R_0}^3$)	diffusion coefficient of water (D_w)
NaPSS	157−375	$(7.38 \pm 2.35) \times 10^{-18}$ cm^2/s	(1.53−1.02) × 10^{-7} (thickness dependent)	(1.3−24) × 10^{-15} cm^2/s (thickness dependent)
PAM	210−450	$(2.26 \pm 0.855) \times 10^{-16}$cm^2/s	$(1.45 \pm 0.12) \times 10^{-13}$	$(1.7 \pm 0.7) \times 10^{-15}$ cm^2/s

interaction term. It was observed that the diffusion coefficient of polyelectrolyte chains was independent of film thickness, whereas the fraction of charged monomer increases linearly with thickness of the films. The swellabilty of the films show the expected dependency on film thickness and was found to be a very sensitive parameter. The diffusion coefficient of the chains was observed to be more than 1 order of magnitude less than that of free neutral polymer chains. The presence of charge within the polymer chains increases the repulsion between chain segments. This interaction makes the chains more expanded on swelling and decreases the mobility of the polyelectrolyte chains when compared to the neutral polymers. The orders of magnitude difference in the repulsive term for polyelectrolyte compared to the neutral polymer demonstrate the importance of the electrostatic interaction in this system.

AUTHOR INFORMATION

Corresponding Author

*E-mail: manabendra.mukherjee@saha.ac.in.

ACKNOWLEDGMENT

Authors thankfully acknowledge Prof. S. Hazra, SPD, SINP, for extending the use of the X-ray reflectivity facility for the study. Authors are thankful to Prof. Koji Nishida of Institute of Chemical Research, Kyoto University, for valuable discussions on polyelectrolytes and introducing NaPSS as an important material.

REFERENCES

(1) Lin, E. K.; Kolb, R.; Satija, S. K.; Wu, W.-L. *Macromolecules* **1999**, *32*, 3753.
(2) Keddie, J. L.; Jones, R. A. L.; Cory, R. A. *Europhys. Lett.* **1994**, *27*, 59.
(3) Zheng, Z.; Kuang, F.; Zhao, J. *Macromolecules* **2010**, *43*, 3165.
(4) Torres, J. M.; Stafford, C. M.; Vogt, B. D. *ACS Nano* **2009**, *3*, 2677.
(5) Jeon, H. S.; Dixit, P. S.; Yim, H. *J. Chem. Phys.* **2005**, *122*, 104707.
(6) Sanchez, I. C. *Physics of Polymer Surfaces and Interfaces*; Butterworth-Heinemann: Boston, MA, 1992.
(7) van Hooy-Corstjeens, C. S. J.; Magusin, P. C. M. M.; Rastogi, S.; Lemstra, P. J. *Macromolecules* **2002**, *35*, 6630.
(8) Wende, C.; Schönhoff, M. *Langmuir* **2010**, *26*, 8352.
(9) Lee, H. J.; Soles, C. L.; Liu, D. W.; Bauer, B. J.; Wu, W. L. *J. Polym. Sci., Part B: Polym. Phys.* **2002**, *40*, 2170.
(10) Silverstein, M. S.; Shach-Caplan, M.; Bauer, B. J.; Hedden, R. C.; Lee, H.-J.; Lande, B. G. *Macromolecules* **2005**, *38*, 4301.
(11) Domack, A.; Johannsmann, D. *J. Appl. Phys.* **1996**, *80*, 2599.
(12) Smith, A. L.; Mulligan, R. B., Sr.; Shirazi, H. M. *J. Polym. Sci., Part B: Polym. Phys.* **2004**, *42*, 3893.
(13) Singh, A.; Mukherjee, M. *Macromolecules* **2003**, *36*, 8728.
(14) Mukherjee, M.; Singh, A.; Daillant, J.; Alain, M.; Cousin, F. *Macromolecules* **2007**, *40*, 1073.
(15) Mondal, M. H.; Mukherjee, M. *Macromolecules* **2008**, *41*, 8753.
(16) Singh, A.; Mukherjee, M. *Macromolecules* **2005**, *38*, 8795.
(17) Mukherjee, M.; Singh, A. *Phys. Status Solidi B* **2007**, *244*, 928.
(18) Nishida, K.; Kaji, K.; Kanaya, T. *J. Chem. Phys.* **2001**, *114*, 8671.
(19) Wang, L.; Bloomfield, V. A. *Macromolecules* **1990**, *23*, 804.
(20) Cohen, J.; Priel, Z.; Rabin, Y. *J. Chem. Phys.* **1988**, *88*, 7111.
(21) Vink, H. *Polymer* **1992**, *33*, 3711.
(22) Fleer, G. J.; Cohen Stuart, M. A.; Scheutjens, J. M. H. M.; Cosgrove, T.; Vincent, B. *Polymers at Interfaces*; Chapman & Hall: London, 1998.
(23) Kowblansky, M.; Zema, P. *Macromolecules* **1982**, *15*, 788.
(24) Dubas, S. T.; Schlenoff, J. B. *Macromolecules* **1999**, *32*, 8153.
(25) Marsh, D. *FEBS Lett.* **1990**, *268*, 371.
(26) Maier, B.; Rädler, J. O. *Phys. Rev. Lett.* **1999**, *82*, 1911.
(27) Maier, B.; Rädler, J. O. *Macromolecules* **2000**, *33*, 7185.
(28) Nishida, K.; Kaji, K.; Kanaya, T. *J. Chem. Phys.* **2001**, *115*, 8217.
(29) Ngai, T.; Wu, C. *Macromolecules* **2003**, *36*, 848.
(30) Crank, J. *The Mathematics of Diffusion*; Celerendon Press: Oxford, 1975.
(31) Vogt, B. D.; Soles, C. L.; Lee, H.-J.; Lin, E. K.; Wu, W.-L. *Langmuir* **2004**, *20*, 1453.
(32) Parratt, L. G. *Phys. Rev.* **1954**, *95*, 359.
(33) Russel, T. P. *Materials Science Reports*; Elsevier Science Publ.: North-Holland: Amsterdam, 1990; Vol. 5.
(34) de Gennes, P. G. *Scaling Concepts in Polymer Physics*; Cornell University Press: Ithaca, NY, 1979.
(35) Strobl, G. R. *The Physics of Polymers: Concepts for Understanding Their Structures and Behavior*; Springer: Berlin, 2007.
(36) Barrat, J.-L.; Joanny, J.-F. *Adv. Chem. Phys.* **1996**, *94*, 1.
(37) Mukherjee, M.; Bhattacharya, M.; Sanyal, M. K.; Geue, Th.; Grenzer, J.; Pietsch, U. *Phys. Rev. E* **2002**, *66*, 061801.
(38) Essafi, W.; Lafuma, F.; Baigl, D.; Williams, C. E. *Europhys. Lett.* **2005**, *71*, 938.
(39) Böhme, U.; Scheler, U. *Adv. Colloid Interface Sci.* **2010**, *158*, 63.
(40) Wang, T.-Y.; Lee, T.-R.; Sheng, Y.-J.; Tsao, H.-K. *J. Phys. Chem. B* **2005**, *109*, 22560.
(41) Qu, D.; Pedersen, J. S.; Garnier, S.; Laschewsky, A.; Möhwald, H.; Klitzing, R. V. *Macromolecules* **2006**, *39*, 7364.
(42) Kraus, J.; Müller-Buschbaum, P.; Kuhlmann, T.; Schubert, D. W.; Stamm, M. *Europhys. Lett.* **2000**, *49*, 210.
(43) Mondal, M. H.; Mukherjee, M.; Kawashima, K.; Nishida, K.; Kanaya, T. *Macromolecules* **2009**, *42*, 732.
(44) Chorny, I.; Dill, K. A.; Jacobson, M. P. *J. Phys. Chem. B* **2005**, *109*, 24056.
(45) Loewenstein, L. M.; Mertens, P. W. *J. Electrochem. Soc.* **1998**, *145*, 2841.
(46) Zhou, K.; Li, J.; Lu, Y.; Zhang, G.; Xie, Z.; Wu, C. *Macromolecules* **2009**, *42*, 7146.